

1
2
3
4
5
6
7
8
9
10
11
12
13
14
15
16
17
18
19
20
21
22
23

**The 23 June 2020, Mw 7.4 La Crucecita, Oaxaca, Mexico earthquake and tsunami: A
Rapid Response Field Survey during COVID-19 crisis**

María-Teresa Ramírez-Herrera^{*}, David Romero, Néstor Corona, Héctor Nava, Hamblet Torija,
Felipe Hernández M.

* Corresponding author full address: Laboratorio de Tsunamis y Paleosismología, Instituto de Geografía, Universidad Nacional Autónoma de México. Av. Universidad 3000, UNAM, Coyocán, Ciudad de México, C.P.04510, tramirez@igg.unam.mx.

Abstract

The 23 June 2020 La Crucecita earthquake occurred at 10:29 hr on the coast of Oaxaca in a Mw 7.4 megathrust event at 22.6 km depth, and triggered a tsunami recorded at Huatulco and Salina Cruz tide gauge stations and a DART off the coast of Mexico. Immediately after the earthquake, a rapid response effort was coordinated by members of the Tsunami and Paleoseismology Laboratory UNAM, despite the challenges by the COVID-19 pandemic crisis, a post-earthquake and post-tsunami field survey went ahead 2 days after the event. We describe here details of the rapid response survey focusing on evidence of vertical coseismic deformation, tsunami, geologic effects, and lessons from working in the field during the COVID-19 crisis. We surveyed 44 km along the coast of Oaxaca focusing on preselected sites. Because of COVID-19 pandemic, some local communities enforced rules of confinement. We solved most of the challenges faced during

24 this crisis by rapid networking with local organizations prior to surveying. We assessed
25 coseismic uplift by means of mortality caused by vertical displacement of intertidal organisms
26 and resurveying of bench marks, and measured tsunami runup using a laser ranger and GPS. Our
27 results show coastal uplift of 0.53 m near the epicenter, decreasing farther away from it, and up
28 to 0.8 m, the latest related to exposure of the coast. Our values of coastal uplift, ca. 0.53 m near
29 the epicenter, fit well with 0.55 m of uplift reported by tide gauge data at Huatulco. Coastal uplift
30 and low tide at the time of the event limited the tsunami inundation and runup on the Oaxaca
31 coast. Nevertheless, we found tsunami inundation evidence at four confined coastal sites
32 reaching a maximum runup of 1.5 m. The enclosed morphology of these sites determined higher
33 runup and tsunami inundation . Local coastal morphology effects are not detected in tsunami
34 models lacking detailed bathymetry and topography. This issue needs to be addressed during
35 tsunami hazard assessments.

36

37 1. Introduction

38

39 *23 June 2020 La Crucecita Earthquake and tsunami*

40

41 The 23 June 2020 La Crucecita earthquake occurred at 10:29 hr (local time), at 15.784° N and
42 96.120° W, and ruptured an estimated 30 km by 20 km (USGS) segment of the Mexican
43 subduction zone along the coast of Oaxaca in a Mw 7.4 megathrust event at 22.6 km deep (SSN,
44 2020), west of the intersection of the Tehuantepec ridge with the trench (Fig. 1). This earthquake
45 triggered a tsunami recorded at Huatulco and Salina Cruz tide gauges (SMN, 2020), and a DART
46 off the coast of Mexico (PTWC, 2020). A tsunami alert by the Pacific Tsunami Warning Center

47 (PTWC) was issued at 10:39 hrs. The earthquake left at least 10 people dead on the Oaxaca
48 highlands and no tsunami damage was reported. Immediately after the earthquake, a rapid
49 response effort was coordinated by members of the Tsunami and Paleoseismology Laboratory,
50 Instituto de Geografía, UNAM and despite the challenges by the COVID-19 pandemic crisis, a
51 post-earthquake and post-tsunami field survey went ahead 2 days after the event. We describe
52 here details of the rapid response survey, challenges faced during a COVID-19 crisis, and results
53 on measurements of coseismic deformation, tsunami runup observations, and other geologic
54 effects generated by the earthquake.
55

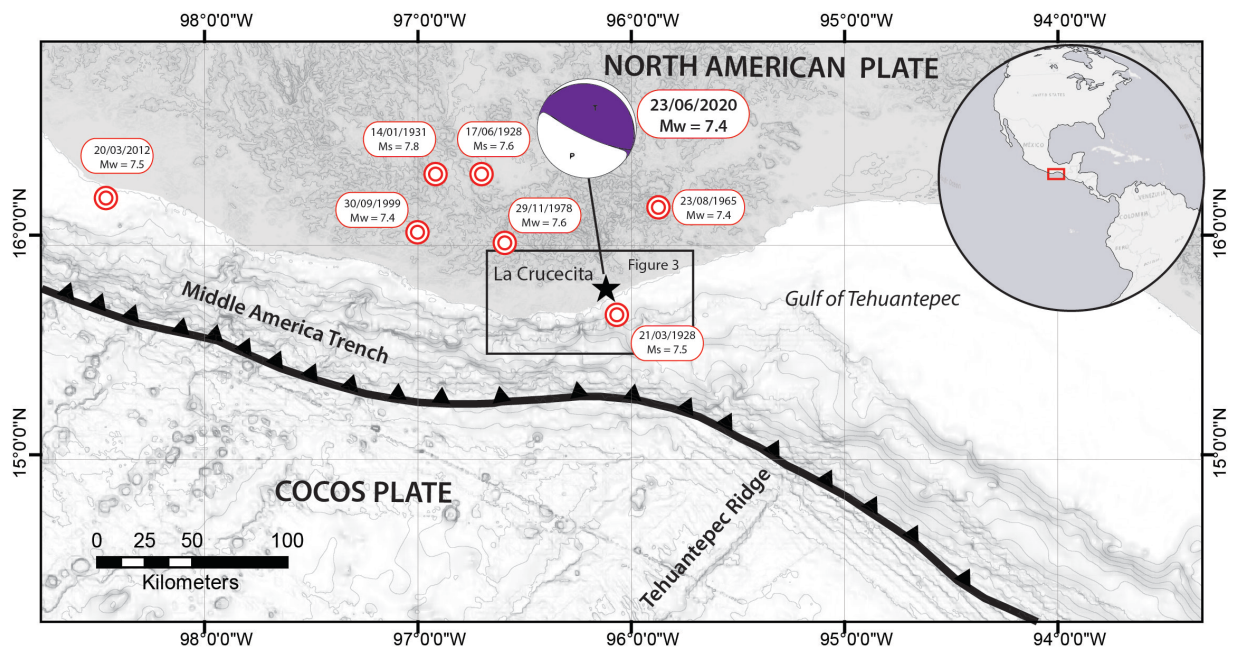


Figure 1. Tectonic and earthquake setting. Red bullseye – $M_w > 7$ earthquakes in the Oaxaca region (SSM, 2020b); star – 23 June 2020 epicenter (SSM, 2020a); Moment tensor of the 23 June 2020 earthquake (USGS (2020)).

56
57 Figure 1. Tectonic and earthquake setting. Red bullseye – $M_w > 7$ earthquakes in the Oaxaca
58 region (SSM, 2020b); star – 23 June 2020 epicenter (SSM, 2020a); Moment tensor of the 23
59 June 2020 earthquake (USGS (2020)).

60

61

62 *Tectonic and earthquake setting*

63

64 The 23 June 2020 La Crucecita earthquake nucleated at the Cocos-North America plate
65 boundary (Fig. 1) with a Mw 7.4 (SSN, 2020a). Convergence rates in this sector of the Mexican
66 subduction zone are near 70 mm/yr (DeMets et al, 2010). The megathrust event (strike= 266.8 ,
67 dip= 17.2, slip= 60.5) reached a maximum slip of 3.2 m slip (SSN, 2020a), although the USGS
68 reported 7.5 m maximum slip (USGS, 2020). The Servicio Mareográfico Nacional (SMN, 2020)
69 reported a +0.55 m land-level change recorded at the HUAT tide gauge. More than 7,000
70 aftershocks were recorded by July 14, 2020, the largest of which had a Mw 5.5 and occurred at
71 21:33 hr on 23 June 2020. Large earthquakes, Mw > 7 , are common in this region and several
72 have been recorded during the last and this centuries (Kostoglodov and Ponce, 1994; Ramírez-
73 Herrera et al., 1999; SSN, 2020b). Earthquakes of this magnitude have rupture areas of about 70
74 x 35 km (length x width) according to the USGS (2020), and earthquakes such as the Mw 6.4,
75 the Puerto Angel earthquake of 1998 produced coastal uplift (Ramírez-Herrera and Zamorano,
76 2002).

77

78 *Tsunami*

79

80 The instrumental record indicates that the 1978 Mw 7.7 (Sanchez and Farreras, 1993) and the
81 2012 Mw 7.5 produced tsunamis (Ramírez- Herrera, personal comm.) (Fig. 1). However,
82 historical events registered in archives indicate that great earthquakes and tsunamis have

4

83 occurred in historical time and geological evidence of the 1787 and probable predecessor in 1537
84 have flooded the southwest coast of Mexico (Ramírez-Herrera et al., 2020). However, because of
85 the short instrumental record, tsunami hazard has been minimized and incorrectly evaluated on
86 the Pacific coast of México.

87

88 *Coastal land level changes and mortality of intertidal organisms*

89

90 Sudden coastal uplift has been documented using mortality of intertidal organisms and upper
91 subtidal algae to estimate coseismic land-level changes particularly in subduction zones (e.g.
92 Plafker, 1964; Johansen, 1971; Bodin And Klinger, 1986 ; Plafker and Ward, 1992; Pelletier et
93 al, 2000; Ortlieb et al., 1996; Ramírez-Herrera and Zamorano, 2002; Lagabrielle et al., 2003;
94 Fariás et al., 2010; Melnick et al., 2012). Vertical zonation of intertidal species depends on
95 factors associated with the tidal cycle (Lunning, 1990; Ortlieb et al. 1996).

96

97 Sudden uplift by earthquakes produces mortality among intertidal organisms, normally life
98 dependent on the time they are exposed during low tides. Intertidal organisms mortality is
99 commonly accompanied by whitening (bleaching) of the dead organism generating a white belt
100 that differentiates clearly from the pinkish color of living organisms right below (Johansen,
101 1971; Ortlieb et al., 1996).

102

103 We used intertidal organisms to evaluate coseismic coastal uplift associated with the 23 June
104 2020 Oaxaca earthquake using coralline algae and invertebrate species living at intertidal and
105 upper subtidal, and in few cases the supralitoral, marine habitats (Ramírez-Herrera & Zamorano

106 2002, Castilla et al. 2010). The intertidal habitat is between the highest and the lowest levels of
107 the tidal range. The biological communities in this habitat may be adapted to be submerged and
108 emerged periodically due the influence of the daily tides. The upper subtidal habitat begins
109 below the lowest level of the intertidal range, and the species inhabiting there are permanently
110 submerged. Supralittoral habitat is submerged only occasionally during the highest spring tides
111 and mainly is influenced by the sea waves and the marine breezes (Tait & Diper 1998).

112

113 *Rapid response*

114

115 The 23 June 2020 earthquake and tsunami occurred during the COVID-19 pandemic crisis,
116 despite this we coordinated a rapid response effort and a post-earthquake and post-tsunami field
117 survey went ahead 2 days after the event. We contacted a local network of people in positions
118 that allowed us rapid access to surveyed sites before the evidence was obliterated by rain and/or
119 human activity.

120

121 2. Field Survey

122

123 Two days after the 2020 Oaxaca earthquake, we started a five-day survey, despite challenges and
124 restrictions imposed by the COVID-19 pandemic, which were related to safe flight travel,
125 confinement, closed hotels and restaurants, to rapidly measure tsunami runup and coastal
126 coseismic deformation, marked by the elevation of bleached intertidal organism belts, and
127 surveying of benchmarks by SMN. We focused at the Huatulco bays region on 15 locations
128 along 44 km of the coast (Fig. 1). The width of bleached intertidal organisms and upper subtidal

129 algae belt, marked by the top and base of the belt, was measured directly on the bleached belt
130 using a metric tape on exposed to waves rocky outcrops and on exposed coral reefs, and only few
131 measurements were made with laser rangefinder when sites were not reachable. We measured
132 tsunami runup by means of marks above the high tide level using a laser rangefinder. Laser
133 rangefinder precision on short distances, < 100 m, is < 5 cm, and measures directly on the
134 exposed rock with tape had less than 0.5 cm error. We photographed all measured sites and
135 located them with a GPS recording time to assess tide levels at the time of measurement. We
136 also surveyed coral reefs using a drone TBS Discovery to map the bleached coral reef areas.

137

138 Tide gauge data from Servicio Mareográfico Nacional (SMN) at Huatulco station (see Table S1
139 of Supplemental material) were used to assess the living position and mortality of intertidal
140 organisms used in this study to estimate coastal uplift.

141

142 3. Observations and results

143

144 *Bleaching or mortality of intertidal organisms*

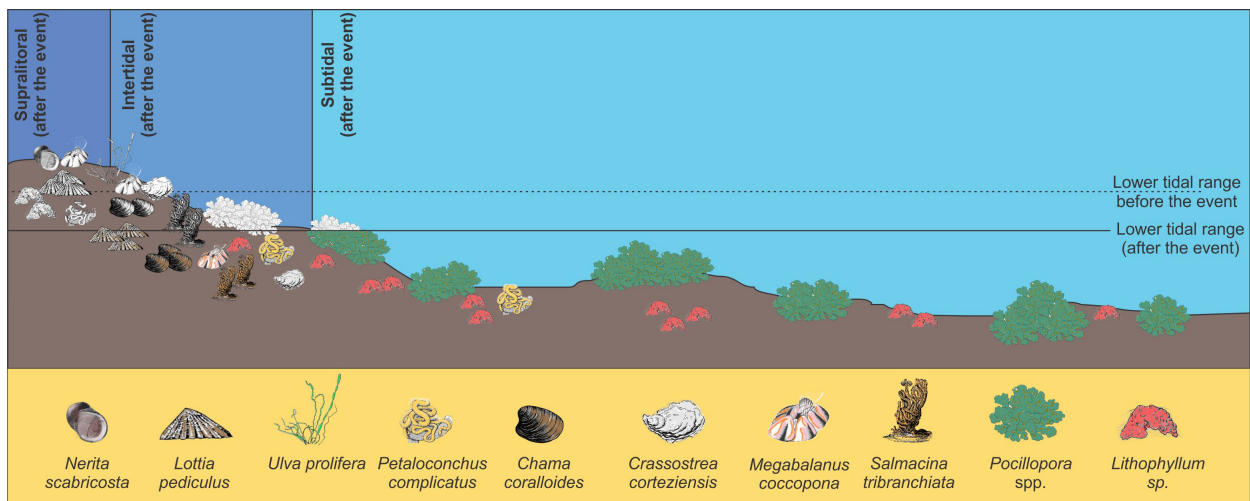
145

146 We identified several species of bleaching organisms and their taxonomy as well as their habitat
147 summarized in Table S2 of the Supplemental material. We also use corals from coral reefs that
148 showed signs of bleaching and emergence. Based on collected samples of organisms and
149 photographs taken in the field, the taxonomic identity of all species were verified with literature
150 available for the area and the World Register of Marine Species (WORMS). Their taxonomy is
151 also summarized in Table S2 and Figure S1 of Supplemental material. In summary, the

7

152 organism identified and used in this study are: a) green algae *Ulva prolifera*, b) gastropod *Nerita*
153 *scabricosta*, c) gastropod *Lottia pediculus*, d) bivalve *Crassostrea corteziensis*, e) vermetid
154 *Petalococonchus complicatus*, f) polychaete *Salmacina tribranchiata*, g) crustacean *Amphibalanus*
155 *eburneus*, h) bivalve *Chama coralloides*, i) crustacean *Megabalanus coccopoma*, j) coralline
156 algae *Lithophyllum* sp., k) stony coral *Pocillopora verrucosa* and l) stony coral *Pocillopora*
157 *damicornis*. Vertical zonation of the organisms used in this study is shown in Figure 2 on and
158 Table S2 of Supplemental material. Mean tidal range is 0.89 m, extreme tidal range is 1.02 m,
159 and maximum extreme tidal range is 1.02 m at this stretch of the Oaxaca coast (Grivel & Grivel,
160 1993).

161



162 Figure 2. Vertical zonation of the organisms used in this study.

163 Figure 2. Vertical zonation of the organisms used in this study

164

165 *Coastal Uplift*

166

167 We measured the bleaching belt of organisms indicative of mortality at 15 locations along the
168 Oaxaca coast (Fig. 3). We collected several measurements at different sites, where possible
169 more than one measurement was registered at each location to have an statistically representative
170 value. Only four sites showed values that did not satisfy the quality criteria (Ortlieb et al., 1996).
171 These values were measured on sites on enclosed tide pools; two high values were measured in
172 an estuary, and one site showed exposed corals difficult to measure from a far distance.

173
174 Our results on measuring the bleaching belt of intertidal organisms indicates that coastal uplift
175 produced by the Mw 7.5 Huatulco earthquake extended along 44 km between San Isidro west of
176 the epicenter, and Barra de la Cruz east of the epicenter (Fig. 3). The further west and east of the
177 epicenter showed low to none evidence of intertidal organisms mortality. The coastal stretch at
178 Playa El Violin, Playa La Yerbabuena, Playa Pescadores-Quinta Real, Fonatur dock, and Playa
179 Pescadores- Santa Cruz showed clear evidence of widespread intertidal organism bleaching belt
180 (OBB). The width of OBB ranged from 0.1 up to 0.8 m along the surveyed area. However, the
181 largest values do not fit the criteria for assessing coastal uplift and are reflecting amplification of
182 the OBB by local features such as coastal morphology (intertidal pools, estuaries, wave splash
183 and far distance features). Those values are excluded from the final estimate of coastal uplift.

184
185 The OBB width at FONATUR dock ranged from 0.4 to 0.54 m, and a mean of 0.47 m (Fig. 3
186 and Fig. 4). At Playa Pescadores-Santa Cruz the OBB width values ranged from 0.5 to 0.56 m
187 with a mean of 0.535 m. We consider these values to be representative of the uplift in this area.
188 At Marina Chahue values range from 0.2 to 0.4, mean value is 0.28 m. We excluded the largest
189 value of 0.8 m because it reflected the amplification of the local intertidal pool. At Playa

190 Pescadores-Quinta Real we measured a relatively high value of 0.6 m. This is caused by the
191 effect of a narrow channel fenced by two breakwater structures on both sides. Further to the NE,
192 at la Bocana, the mean value of OBB width was 0.37 m. At Zimatan-Laguna Las Garzas beach,
193 values range from 0.2 to 0.3 m., which reflects the decrease in uplift away from the area of the
194 epicenter. At Zimatan-Laguna Las Garzas river mouth, values were high, mean value 0.77 m.
195 This site does not reflect the real deformation because the vertical distribution of intertidal
196 organisms here is influenced by specific characteristics of the location (Ortlieb et al, 1996). At
197 Barra de La Cruz, we were not granted access to the beach due to COVID-19 lockdown
198 measures taken by the locals. To the west of the epicenter, at Playa Yerbabuena (SEMAR)
199 values ranged from 0.2 to 0.53 m, with a mean value of 0.32 m. Playa Violin showed OBB
200 width ranged from 0.29 to 0.57 m, mean value is 0.42 m (Fig. 3 and Fig. 4). At Bahía El Órgano,
201 representative values ranged from 0.2 to 0.4 m. We did not include an extremely high value of
202 0.8 m produced by the local site effect (an enclosed tidal pool). Playa Riscalillo showed coral
203 reef bleached width ranging between 0.10 to 0.20 m. San Agustin bay also showed coral reef
204 exposed above mean sea level, however the distance to the reef precluded us from taking a
205 precise measure, thus we excluded the 0.70 m value that is not representative. At Playa del Amor
206 values ranged from 0.10 to 0.20 m which are consistent with an expected decrease of OBB width
207 away from the epicenter. The furthest west location, at San Isidro evidence was scarce and the
208 belt measured at the mouth of an estuary showed values in between 0.15 and 0.20 m, reflecting
209 site increment effects. The latest suggests that uplift here was minimal, perhaps less than a few
210 centimeters. We did not expect to find evidence further to the west since last site only showed
211 patchy evidence of OBB.

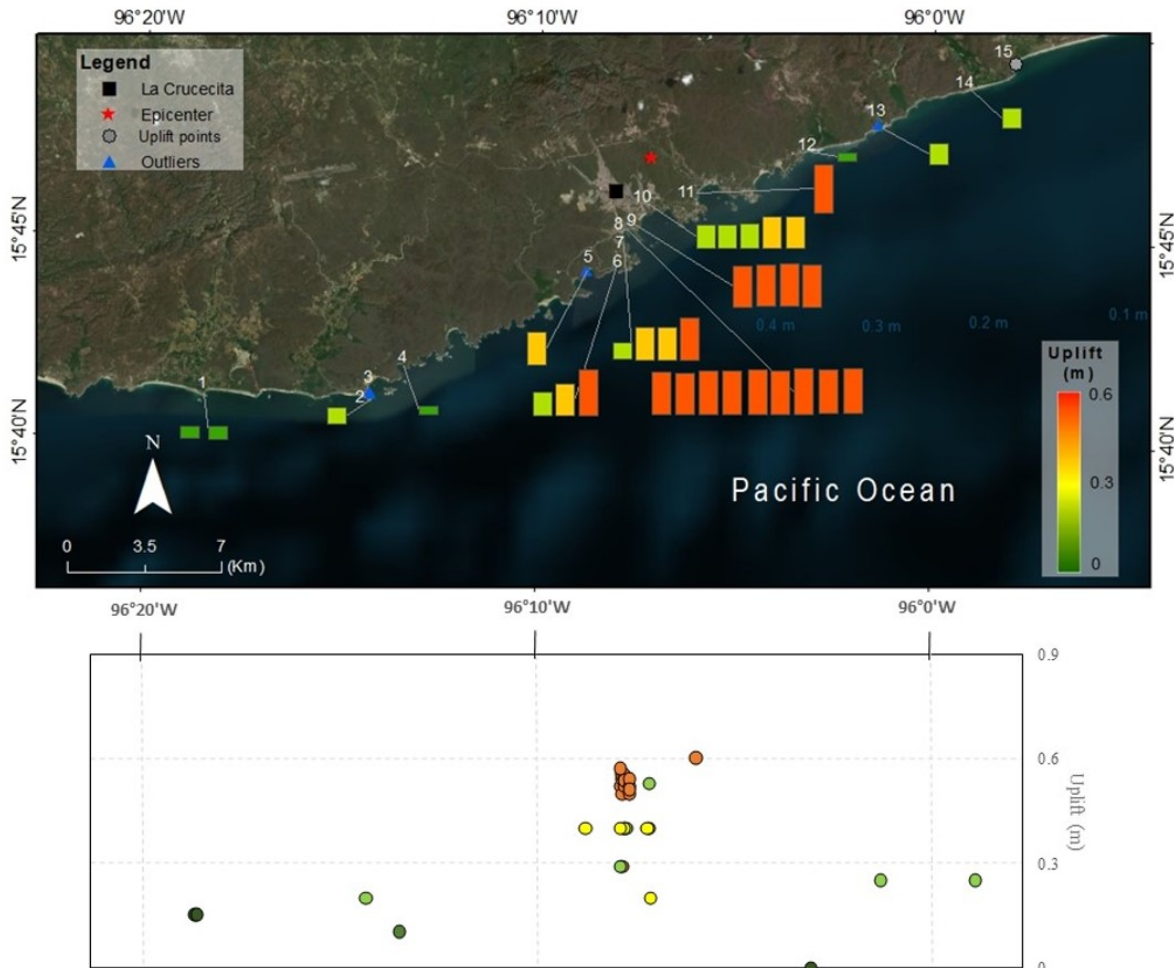


Figure 3. Coseismic uplift generated by the La Crucecita Mw 7.4, 23 June 2020, earthquake. Bars indicate the width (m) of the organisms bleached belt (OBB) at 15 locations along 44 km of coastal stretch: 1. San Isidro, 2. Playa del Amor, 3. San Agustín, 4. Bahía Riscalillo, 5. Playa el Órgano, 6. Playa el Violín, 7. Playa Yerbabuena – SEMAR, 8. Playa Pescadores, 9. Fonatur dock, 10. Marina Chahué, 11. Playa Pescadores – Quinta Real, 12. La Bocana Río Copalita, 13. Río Zimatán, 14. Zimatán – Laguna las Garzas, 15. Barra de la Cruz. Blue triangles – sites with values > 0.5 m. Please see the text for explanation.

212

213 Figure 3. Coseismic uplift generated by the La Crucecita Mw 7.4, 23 June 2020, earthquake.

214 Bars indicate the width (m) of the organisms bleached belt (OBB) at 15 locations along 44 km of

215 coastal stretch: 1. San Isidro, 2. Playa del Amor, 3. San Agustín, 4. Bahía Riscalillo, 5. Playa el

216 Órgano, 6. Playa el Violín, 7. Playa Yerbabuena – SEMAR, 8. Playa Pescadores, 9. Fonatur

217 dock, 10. Marina Chahué, 11. Playa Pescadores – Quinta Real, 12. La Bocana Río Copalita, 13.

218 Río Zimatán, 14. Zimatán – Laguna las Garzas, 15. Barra de la Cruz. Blue triangles – sites with
219 values > 0.5 m. Please see the text for explanation.

220

221 Figure 3 summarizes the distribution and amount of coseismic uplift estimated from OBB. We
222 have used all values and mean values to graphically represent the width of the OBB. These
223 values are estimates of the land level change, i.e. coseismic uplift by the 23 June 2020
224 earthquake. We use only values that best represent the uplift and excluded values from locations
225 that were influenced by site effects. The maximum estimated uplift was identified at Playa
226 Pescadores- Santa Cruz, FONATUR dock, Playa Pescadores-Quinta Real, and Playa El Violin.
227 From this area on, to the west and northeast farther away from the earthquake epicenter, values
228 of uplift tend to decrease. Uplift represented by mortality of intertidal organisms extended about
229 40 km along the coast. We are not sure about the extent of uplift further NE since we were
230 prevented access to locations from Barra de La Cruz on, however we already observed a
231 decrease in uplift at the nearest location. The general pattern of coseismic uplift indicated by the
232 OBB width suggests greater land vertical motion closer to the epicenter.

233

234 We measured the elevation of two benchmarks set by the SMN to have a different data parameter
235 and being able to compare and determine with more parameters land-level changes. The first
236 bench mark (BN20HUA01) is located at the Fonatur dock next to the tide gauge and the second
237 bench at the park kiosk (BN20HUA02). Bench mark BN20HUA01 showed 0.528 m uplift and
238 BN20HUA02 experienced 0.491 m uplift after the 23 June 2020 earthquake.

239

240 *Tsunami*

241
242 A tsunami was generated by the Mw 7.4 La Crucecita earthquake. The earthquake occurred at
243 10:29 hr local time. The SMN Huatulco tide gauge registered a maximum tsunami amplitude of
244 0.61 m at 13:12 hr local time, and at Salina Cruz tide gauge station with a maximum amplitude
245 of 1.394 m at 12:34 hr local time (Fig. S2 Supplemental material). According to the registered
246 tide gauge data, the sea started retreating at 10:30 hr reaching a maximum retreat of -1.273 m at
247 10:36 hr. The SMN Huatulco interpretation suggests that the tsunami initiated at 11:12 hr
248 reaching a maximum amplitude of 0.61 m at 13:12 hr, and ending at 18:06 hr (Fig. S2
249 Supplemental material)

250
251 However, we observed several videos recorded by static camera devices at the FONATUR dock
252 and estimated that the sea started to retreat approximately 5 to 7 minutes after the earthquake (the
253 retreat could have started earlier since power went off and 5 minutes of record were lost), with
254 turbulence and sediment in suspension, and reached the lowest level 11 minutes after the
255 earthquake. The sea apparently made a return, with relative strong energy and speed, 13 minutes
256 after the earthquake, i.e. at approximately between 10:43 or 10:45 hr local time. At 10:47 again
257 the sea retreated and reached a maximum height by 10:48 hr to again reach an apparent lower
258 level than the one the sea showed before the earthquake.

259
260 According to social media and witnesses reports, the sea retreated almost immediately after the
261 earthquake but did not cause extensive inundation nor damage was reported in coastal cities.
262 Witnesses reported sea return but emphasized it never reached the sea level previous to the
263 earthquake. After the earthquake some coastal residents started a timely evacuation to higher

264 ground after seeing the sea retreat, however not all coastal residents evacuated. No damage nor
265 deaths were reported due to the tsunami. The Mexican Tsunami Warning Center (CAT – Centro
266 de Alertas de Tsunami) issued a tsunami alert, however none of the coastal residents we
267 interviewed were aware of the tsunami warning other than the earthquake itself.
268
269 Tsunami marks left on the shore were scarce on the surveyed sites. We expected to find only a
270 few marks after looking at tide gauge data reports of the 23 June 2020 tsunami on Huatulco and
271 Salina Cruz stations, also because at the time of earthquake and tsunami the tide level was low (-
272 0.582 m), and as explained above we observed a bleaching belt of intertidal organisms
273 indicative of coastal uplift. However, we located sand and cobbles beyond high tide mark on
274 boat ramps, organic debris (broken coral) higher than the highest tide mark on a beach, and other
275 organic debris, at four sites along 44 km of the surveyed coast. At Playa El Violin we found a
276 line of broken corals from a local coral reef located higher than the highest tide mark, indicative
277 of tsunami runup ~ 0.9 m. This narrow and confined bay faces to the SW (Fig. 5). The second
278 site at Marina Chahue, with a very narrow entrance to the Marina (Fig. 5), showed a tsunami
279 mark made of sand and cobbles on a concrete ramp next to fuel pumps, and the measured runup
280 was ~1.07 to 1.37 m. Playa Pescadores (Quinta Real) is an extremely narrow channel facing SE,
281 confined by groins that might have increased the tsunami runup up to ~1.57 m. La Yerbabuena
282 beach at the boat ramp, confined by a dock and a cliff, also showed a tsunami mark made of
283 sand and cobbles with a runup of 0.99 m (Fig. 5). All these sites have in common being narrow
284 and confined. We explained the absence of tsunami marks by: 1) low tide at the time of tsunami
285 and 2) land uplift of this portion of the coast caused by the earthquake, that decreased the size of
286 the tsunami. The few tsunami marks left on the shore can be explained by the local morphology

287 of these sites: very narrow confined channels and likely the bathymetry of a narrow entrance bay.
288 These local effects cannot be envisaged in tsunami models due to the gross topography
289 bathymetry used in modeling, and this is an issue that requires to be addressed when using
290 modeling in tsunami hazard assessment.

291

292 *Other Geologic effects (liquefaction, fissures, landslides)*

293

294 We observed near the coast several geologic effects associated with the Mw 7.4 earthquake's
295 ground shaking, with PGA 20% g and PGV 41.4 cm/s, intensity VIII near the epicenter (USGS,
296 2020) (Fig. 1). Rockfalls and landslides were common along coastal highways and on some
297 slopes, however their size was relatively small. Lateral spreading, fissures on the ground and
298 beaches were common. Liquefaction (sand boils) was focused near estuaries, river mouths, and
299 lagoons (Fig. 6). Most of the landslides were reported on the Oaxaca highlands and these were
300 not included in the scope of this survey. It is worth mentioning that the current rainy season at
301 the time of the earthquake in Oaxaca, Mexico, most probably increased slope failures.

302

303 Buildings along the coast apparently had very few damage. Although beyond the scope of this
304 survey, we noticed mainly a few 3 to 4-store buildings that showed structural damage. Most of
305 the hotels and houses close to the beach responded well with minor damage (broken roof tiles).

306

307 *Surveying during COVID-19 crisis*

308

309 Field survey was carried out in the state of Oaxaca during the COVID-19 pandemic crisis. Santa
310 María Huatulco was selected as the operation center, since this was the area of the La Crucecita
311 earthquake epicenter. On the arrival day, the epidemiological panorama of the coastal region
312 showed 170 COVID-19 active cases, and at Santa María Huatulco only 7 COVID-19 cases. We
313 followed all recommendations regarding prevention during the course of the post-earthquake and
314 tsunami survey: all the participants involved wore masks, the use of alcohol gel, frequent hand
315 washing and keeping a 1.5 m distance. Only one vehicle was used during the survey, which was
316 washed and disinfected every day, the interaction with people during field work was always
317 respecting a safe distance and the use of masks, in addition to the permanent vigilance for the
318 appearance of any symptoms by the team members (Fig. 7).

319
320 We faced a few challenges and restrictions imposed by the COVID-19 pandemic. Prior to
321 traveling we contacted our local network in Huatulco, Oaxaca, to rapidly get access to sites along
322 the coast. Traveling to the coast in a rapid way required flying in a packed airplane with no
323 empty seats in between passengers. Due to the confinement in some towns most hotels and
324 restaurants were closed, however we had the support of the La Crucecita, Huatulco, Firemen
325 (Bomberos de Oaxaca), and FONATUR (the Federal office for tourist affairs) who kindly
326 arranged for us to use a truck and hotel reservations during the survey. To get rapid access to less
327 accessible sites, the Navy local office aided in using a Navy boat (Fig. 7). All of this was
328 arranged previous to arrival by our local contact with Oaxaca Firemen. It is therefore very
329 important to have a good network and work with locals in times of crisis for a rapid evaluation of
330 earthquake and tsunami effects.

331

332 During the survey, we always respected the local practices and actions of containment because of
333 the pandemic. We first talked with the local authorities at checkpoints to ask for access, as it was
334 the case in the community of La Bocana and Copalita. However, we could not have access to
335 some places, such as the community of Barra de La Cruz where access to anyone outside the
336 community was prohibited (Figure 7). We solved this situation by visiting the nearest possible
337 site to make observations.

338

339 Summary and Discussion

340

341 The 23 June 2020 La Crucecita earthquake produced coastal uplift recorded by the extent of
342 mortality of intertidal organisms caused by sudden vertical motions. A white belt of dead
343 organisms appeared at several sites along the coast and was already visible by the second day
344 after the earthquake. The width of this belt varied along the coast, generally showing higher
345 values near the epicenter and decreasing further away. Evidence of coastal deformation was
346 observed between San Isidro and Zimatán (Fig. 3), that we considered the along-strike extent of
347 the 23 June 2020 La Crucecita earthquake rupture of ca. 40 km. Our results based on the
348 interpretation of most representative values that fulfilled the criteria explained above, show
349 coastal coseismic uplift of 0.53 m near the epicenter and farther away decreasing to 0.10 m. The
350 bleached belt of intertidal organisms is a reliable estimate of the uplift produced by the 23 June
351 2020 La Crucecita earthquake. Other phenomena such as extremely low tide and El Niño events
352 cannot explain the mortality of intertidal organisms since, firstly we surveyed sites that had
353 experienced low tide sequences and 2020 had no El Niño event on the coast of México.

354 Furthermore, fishermen and locals pointed to the “no return of the sea to its normal level after the

355 earthquake”, i.e. coastal land level change, and to the mortality of coral reefs and other intertidal
356 organisms. Furthermore, we corroborated our results with measurements of two geodetic SMN
357 benchmarks at Santa Maria Huatulco near la Crucecita. Our results using benchmarks height
358 measurements confirm coastal uplift of 0.528 m on the coast and 0.491 m slightly inland (Fig. 3).
359 Also, we used the SNM tide gauge data (Fig. S1 of Supplemental material) and SNM report that
360 indicates coastal uplift of 0.55 m. Therefore the observed bleached belt reliably represents
361 coseismic uplift produced by the 23 June 2020 La Crucecita earthquake. We suggest that the use
362 of organisms sudden mortality aids in a rapid survey of earthquake deformation along the coast.

363
364 Tsunami evidence was scarce and our measurements of tsunami runoff on the surveyed coastal
365 stretch showed 0.9 m and a maximum runoff of 1.5 m at four confined coastal sites. The scarcity
366 of tsunami evidence can be explained by several factors. Firstly, it was raining during and the
367 night after the event, thus evidence such as debris are not perennial and could be easily washed
368 away by rain. Secondly, the tide level at the tsunami arrival was low (-0.58 m), which also
369 contributed limited tsunami inundation and runoff at the coast. Finally, coastal uplift of ca. 0.53
370 to 0.10 m, also limited tsunami inundation and runoff. Despite all of the explained above, we
371 observed evidence at four coastal sites with confined coastal morphology. Tide gauge records,
372 testimonies by locals, and video recordings also support evidence of the sea retreat and energetic
373 sea return, even if with relatively low tsunami heights, a few minutes (~5 to 7 minutes) after the
374 earthquake.

375
376 Thus, it is important to remember and emphasize that historical and prehistorical earthquakes
377 produced great tsunamis on the Mexican Pacific coast, such as the 1787 event and the possible

378 predecessor of 1537 (Ramírez-Herrera et al., 2020). Instrumental data unfortunately do not
379 capture in their short record (ca. 100 years) in Mexico all tsunamigenic events, nor all
380 earthquakes produced coastal uplift on the Pacific coast of Mexico. For instance, the 1995 Mw
381 8.0 Colima-Jalisco earthquake produced coastal subsidence and a significant tsunami with run-up
382 height of 5.1 m (e.g. Pacheco et al., 1997; Borrero et al., 1997; Trejo-Gómez et al., 2015). Even
383 when earthquakes produced coastal uplift, as it happened during the 19 September 1985 Mw 8.1
384 (Bodin and Klinger, 1986) and 20 September 1985 Mw7.5 earthquakes, two tsunamis flooded
385 the coast of Michoacan and Guerrero, Mexico (Sanchez and Farreras, 1993) leaving geologic
386 evidence (Ramírez-Herrera et al., 2012). It is also possible that shallow events near the trench
387 might cause coastal subsidence and large tsunamis such as the 1787 event (Ramírez-Herrera et
388 al., 2020) and the more recent 1995 Mw 8.0 Colima-Jalisco earthquake (Pacheco et al., 1997;
389 Hjörleifsdóttir et al., 2018). Tsunami modeling exercises may aid in estimating tsunami
390 amplitudes, however due to the lack of detailed bathymetry and topography, local coastal
391 morphology effects are missed in models. Thus an effort should be made to produce bathymetric
392 data near the coast to have reliable tsunami models. This and tsunami education programs are of
393 most importance in tsunami hazard prevention to create tsunami resilient coastal communities.
394
395 Finally, our lesson from working during the Covid-19 pandemic crisis is that it is crucial to have
396 a local network of collaborators who facilitate a rapid response during post-earthquake and
397 tsunami surveys by aiding in getting access to localities and sites affected by this phenomena,
398 assists in logistics, help in understanding and respecting local practices by communities that in
399 turn cooperate in describing these phenomena.

400

401 Data and Resources

402 Supplemental material includes Table S1 presenting tide gauge data from Servicio Mareográfico
403 Nacional (SMN) at Huatulco station. Data were used to assess living position and mortality of
404 intertidal organisms.

405

406 Table S2 provides data on the taxonomic identity and vertical zonation of organisms used in this
407 study.

408

409 Figure S1 includes details, taxonomy, and photographs of the organisms used in this study.

410 Figure S2 shows the Huatulco tide gauge data interpretation of land-level vertical displacement
411 and tsunami amplitude after the 23 June 2020 earthquake.

412

413 *Acknowledgments*

414

415 This work was supported by Instituto de Geografía, Universidad Nacional Autónoma de México
416 and CONACYT-SEP 284365 granted to Ramírez-Herrera. We thank the following people and

417 Institutions for logistic help during the survey: Bomberos Oaxaca - Lic. Manuel A. Maza

418 Sánchez; Secretaria de Marina - Sector Naval Huatulco- Contralmirante CGDEM Procoro Juan

419 Trinidad García and Capitán Juan Solís Guillén, Secretaría de Seguridad Pública- Lic. Raul

420 Ernesto Salcedo Rosales; Secretaria de Turismo - Delegación Regional Huatulco - Lic. Raúl

421 Sinobas Solís, Fonatur - Delegación regional CIP Huatulco - Ing. Ramón Sinobas Solís,

422 Capitanía del Muelle de Cruceros – Cap. Ángulo, FONATUR – Mario Harrigan. Víctor Vargas

423 helped with figure drafting. Diego Melgar shared preliminary slip, vertical deformation, and

424 tsunami amplitude models. We thank the coastal communities of Oaxaca visited during this post-
425 earthquake and post-tsunami field survey for kindly giving access, sharing their memories and
426 videos of the events.

427

428 **References**

429

430 Bodin, P., & Klinger, T. (1986). *Coastal uplift and mortality of intertidal organisms caused by*
431 *the September 1985 Mexico earthquakes*. *Science*, 233, 1071–1073.

432 Borrero, J., Titov V., Ortiz M., , Synolakis C. (1997). Mexican Earthquake Generates Tsunami,
433 New Data, and Unusual Photos. *Earth in Space*, vol. 9, no. 7, p. 5-8, 1997 American
434 Geophysical Union. Retrieved July 21, 2020
435 from http://www.agu.org/sci_soc/eisborerro.html

436 Castilla, J. C., Manríquez, P. H., & Camaño, A. (2010). Effects of rocky shore coseismic uplift
437 and the 2010 Chilean mega-earthquake on intertidal biomarker species. *Marine Ecology*
438 *Progress Series*, 418, 17-23.

439 DeMets, C., Gordon, R. G., & Argus, D. F. (2010). Geologically current plate motions.
440 *Geophysical Journal International*, 181(1), 1–80.

441 Fariás, M., Vargas, G., Tassara, A., Carretier, S., Baize, S., Melnick, D., & Bataille, K. (2010).
442 Land-level changes produced by the 2010 Mw8. 8 Chile earthquake. *Science*, 329, 916.

- 443 Grivel, P. F., & Grivel, F. V. (1993). Tablas de Predicción de mareas 1993. Puertos del Pacífico.
444 *Servicio Mareografico Nacional. UNAM*, 115.
- 445 Hjörleifsdóttir V. Sánchez Reyes H. S. Ruiz Angulo A. Ramírez-Herrera M. T. Castillo-Aja R.
446 Singh S. K., and Ji C. 2018. Was the October 9th 1995 Mw 8 Jalisco, Mexico earthquake a
447 near trench event? *J. Geophys. Res.* doi: [https://doi-](https://doi-org.pbidi.unam.mx:2443/10.1029/2017JB014899)
448 [org.pbidi.unam.mx:2443/10.1029/2017JB014899](https://doi-org.pbidi.unam.mx:2443/10.1029/2017JB014899).
- 449 Johansen, H. W. (1971). Effects of elevation changes on benthic algae in Prince William Sound.
450 *In :The Great Alaska Earthquake of 1964, Washington, D.C.: National Academy of*
451 *Sciences*, p.35-68.
- 452 Kostoglodov, V., & Ponce, L. (1994). Relationship between subduction and seismicity in the
453 Mexican part of the Middle America trench. *Journal of Geophysical Research*, 99, 729–
454 742.
- 455 Lagabrielle, Y., Pelletier, B., Cabioch, G., Régnier, M., & Calmant, S. (2003). Coseismic and
456 long-term vertical displacement due to back arc shortening, central Vanuatu: Offshore and
457 onshore data following the Mw 7.5, 26 November 1999 Ambrym earthquake. *Journal of*
458 *Geophysical Research*, 108, 2519.
- 459 Luning, K. S. (1990). *Their environment, Biogeography and Ecophysiology*. New York: John
460 Wiley & Sons, Inc. 527p.
- 461 Melnick, D., Cisternas, M., Moreno, M., & Norambuena, R. (2012). Estimating coseismic
462 coastal uplift with an intertidal mussel: calibration for the 2010 Maule Chile earthquake

- 463 (Mw= 8.8). *Quaternary Science Reviews*, 42, 29–42, ISSN 0277-3791.
464 <https://doi.org/10.1016/j.quascirev.2012.03.012>
- 465 Ortlieb, L., Barrientos, S., & Guzman, N. (1996). Coseismic coastal uplift and coralline algae
466 record in northern Chile: the 1995 Antofagasta earthquake case. *Quaternary Science*
467 *Reviews*, 15, 949–960.
- 468 Pacheco, J., Singh, S. K., Domínguez, J., Hurtado, A., Quintanar, L., Jiménez, Z., Yamamoto, J.,
469 Gutiérrez, C., Santoyo, M., & Bandy, W. (1997). The October 9, 1995 Colima-Jalisco,
470 Mexico earthquake (Mw 8): An aftershock study and a comparison of this earthquake with
471 those of 1932. *Geophysical Research Letters*, 24, 2223–2226.
- 472 Pacific Tsunami Warning Center. (2020). *ITIC Tsunami Bulletin Board Tsunami, NWs Pacific*
473 *Tsunami Warning Center Bulletin Jun 23 2020, NOAA*. Accessed 23 June 2020.
- 474 Pelletier, B., Régnier, M., Calmant, S., Pillet, R., Cabioch, G., Lagabrielle, Y., Bore, J.-M.,
475 Caminade, J.-P., Lebellegard, P., & Cristopher, I. (2000). Le séisme d’Ambrym–Pentecôte
476 (Vanuatu) du 26 novembre 1999 (Mw: 7, 5): données préliminaires sur la sismicité, le
477 tsunami et les déplacements associés. *Comptes Rendus de l’Académie Des Sciences-s-Series*
478 *IIA-e-Sciences de 10 Terre et Des Planetes*, 331(1), 21–28.
- 479 Plafker, G. (1964). Tectonic deformation associated with the 1964 Alaska earthquake. *Science*,
480 148(3678), pp.1675-1687.

- 481 Plafker, G., & Ward, S. N. (1992). Backarc thrust faulting and tectonic uplift along the
482 Caribbean Sea Coast during the April 22, 1991 Costa Rica earthquake. *Tectonics*, *11*, 709–
483 718.
- 484 Ramírez-Herrera, M.-T., Corona, N., Cerny, J., Castillo-Aja, R., Melgar, D., Lagos, M.,
485 Goguitchaichvili, A., Machain, M. L., Vazquez-Caamal, M. L., Ortuño, M., Caballero, M.,
486 Solano-Hernandez, E., & Ruiz-Fernández, A. (2020). Sand deposits reveal great
487 earthquakes and tsunamis at Mexican Pacific Coast. *Scientific Reports*, *10*, 11452.
488 <https://doi.org/10.1038/s41598-020-68237-2>
- 489 Ramirez-Herrera, M.-T., Kostoglodov, V., Summerfield, M. A., Urrutia-Fucugauchi, J., &
490 Zamorano, J. J. (1999). A reconnaissance study of the morphotectonics of the Mexican
491 subduction zone. *ZEITSCHRIFT FUR GEOMORPHOLOGIE SUPPLEMENTBAND*, 207–
492 226.
- 493 Ramírez-Herrera, M.-T., Lagos, M., Hutchinson, I., Kostoglodov, V., Machain, M. L., Caballero,
494 M., Goguitchaichvili, A., Aguilar, B., Chagué-Goff, C., Goff, J., Ruiz-Fernández, A., Ortiz,
495 M., Nava, H., Bautista, F., Lopez, G. ., & Quintana, P. (2012). Extreme wave deposits on
496 the Pacific coast of Mexico: Tsunamis or storms?—A multi-proxy approach.
497 *Geomorphology*, *139*, p.360-371. <https://doi.org/10.1016/j.geomorph.2011.11.002>
- 498 Ramirez-Herrera, M.-T., & Orozco, J. J. Z. (2002). Coastal uplift and mortality of coralline algae
499 caused by a 6.3 Mw earthquake, Oaxaca, Mexico. *Journal of Coastal Research*, *18*, 75–81.

500 Sánchez Devora, A. J., & Farreras Sanz, S. (1993). *Catalog of tsunamis on the western coast of*
501 *Mexico. Rep SE-50.*(World Data Center A for Solid Earth Geophysics, NOAA, National
502 Geophysical Data Center, Boulder, Colorado, 1993).

503 Servicio Mareográfico Nacional, 2020. Reporte del tsunami producido por el sismo de magnitud
504 7.5 ocurrido el día 23 de junio
505 de 2020 al sureste de Crucecita, Oaxaca. UNAM, México
506 http://www.mareografico.unam.mx/portal/docu/Pdfs/Reporte_Servicio_Mareografico_23_junio_2020.pdf
507

508 Servicio Sismológico Nacional (SSN) (2020a) Reporte Especial - Sismo del 23 de Junio de 2020,
509 Costa de Oaxaca (M 7.5). IGEF - UNAM, México.
510 ([http://www.ssn.unam.mx/sismicidad/reportes-](http://www.ssn.unam.mx/sismicidad/reportes-especiales/2020/SSNMX_rep_esp_20200623_Oaxaca-Costa_M75.pdf)
511 [especiales/2020/SSNMX_rep_esp_20200623_Oaxaca-Costa_M75.pdf](http://www.ssn.unam.mx/sismicidad/reportes-especiales/2020/SSNMX_rep_esp_20200623_Oaxaca-Costa_M75.pdf))

512 Servicio Sismológico Nacional (SSN). (2020b). *Catálogo de Sismos.*
513 <http://www2.ssn.unam.mx:8080/catalogo/> (Last Accessed June 25, 2020).

514 Tait, R. V., & Dipper, F. (1998). *Elements of marine ecology.* Butterworth-Heinemann.

515 Trejo-Gómez, E., Ortiz, M., & Núñez-Cornú, F. J. (2015). Source Model of the October 9, 1995
516 Jalisco-Colima Tsunami as constrained by field survey reports, and on the numerical
517 simulation of the tsunami. *Geofisica Internacional*, 54(2), 149–159.

518 USGS. (2020). *M 7.4 - 9 km SE of Santa María Xadani, Mexico.*

519 <https://earthquake.usgs.gov/earthquakes/eventpage/us6000ah9t/ground-failure/summary>

520 *Full mailing address for each author*

521

522 María Teresa Ramírez-Herrera, Laboratorio de Tsunamis y Paleosismología, Instituto de
523 Geografía, Universidad Nacional Autónoma de México. Av. Universidad 3000, UNAM,
524 Coyocán, Ciudad de México, C.P.04510, tramirez@igg.unam.mx

525

526 David Romero H. Facultad de Ciencias, Universidad Nacional Autónoma de México. Av.
527 Universidad 3000, UNAM, Coyocán, Ciudad de México, C.P.04510,
528 dromeroh@ciencias.unam.mx

529

530 Néstor Corona Morales, Centro de Estudios en Geografía Humana-El Colegio de Michoacán,
531 Cerro de Nahuatzen 85, Fracc. Jardines del Cerro Grande, La Piedad, Mich., México, C.P.59379,
532 corona@colmich.edu.mx

533

534 Hector Nava, Dep. de Zoología. Instituto de Investigaciones sobre los Recursos Naturales.
535 Universidad Michoacana de San Nicolás de Hidalgo. Av. San Juanito Itzícuaró S/N, Nueva
536 Esperanza, Morelia Mich. México., C.P.58337, hector.nava@umich.mx

537

538 Hamblet Torija Morales, H. Cuerpo de Bomberos Oaxaca- Blvd. Chahue 1 sector H2, 70980
539 Santa Cruz Huatulco, Oaxaca, Mx, hamblettorija@gmail.com

540

541 Felipe Hernández Maguey, Instituto de Geofísica, UNAM, Circuito de la Investigación
542 Científica s/n, Ciudad Universitaria, Coyoacán, C.P.04510, Ciudad de México,
543 fhmaguey@igeofisica.unam.mx

544

545 **List of Figure Captions**

546

547 Figure 1. Tectonic and earthquake setting. Red bullseye – $M_w > 7$ earthquakes in the Oaxaca
548 region (SSM, 2020b); star – 23 June 2020 epicenter (SSM, 2020a); Moment tensor of the 23
549 June 2020 earthquake (USGS (2020)).

550

551 Figure 2. Vertical zonation of the organisms used in this study.

552

553 Figure 3. Coseismic uplift generated by the La Crucecita M_w 7.4, 23 June 2020, earthquake.
554 Bars indicate the width (m) of the organisms bleached belt (OBB) at 15 locations along 44 km of
555 coastal stretch: 1. San Isidro, 2. Playa del Amor, 3. San Agustín, 4. Bahía Riscalillo, 5. Playa el
556 Órgano, 6. Playa el Violín, 7. Playa Yerbabuena – SEMAR, 8. Playa Pescadores, 9. Fonatur
557 dock, 10. Marina Chahué, 11. Playa Pescadores – Quinta Real, 12. La Bocana Río Copalita, 13.
558 Río Zimatán, 14. Zimatán – Laguna las Garzas, 15. Barra de la Cruz. Blue triangles – sites with
559 values > 0.5 m. Please see the text for explanation.

560

561 Figure 4. Mortality of intertidal organisms caused by sudden land uplift shown by a bleaching
562 belt of intertidal organisms. UL = Upper limit and LL Lower limit of organism bleached belt.

563 a) La Bocana Río Copalita , b) San Isidro, c) Bahía Riscalillo – aerial view of patches of

564 bleached coral reef, d) Marina Chahué, e) Playa el Violín, f) Bleached coral reef at Bahía
565 Riscalillo g) Playa Yerbabuena – SEMAR – bleached coral, h) Playa Pescadores, i). Detail of
566 bleached belt at Playa Pescadores.

567

568 Figure 5. Tsunami runup marked by debris at four locations along the study area. a) El Violín
569 Beach, b) Marina Chahué, c) Playa Yerbabuena – SEMAR.

570

571 Figure 6. Other Geologic effects: liquefaction, fissures, landslides caused by La crucecita
572 earthquake of 23 June 2020. a) Playa Pescadores – Quinta Real, b), c) y g) Zimatán-Laguna las
573 Garzas, d) La Bocana Río Copalita, e), f) Boulevard Chahué.

574

575 Figure 7. Surveying during COVID-19 crisis

576

577 **Supplemental material**

578

579 Table S1. Tide gauge data from Servicio Mareográfico Nacional (SMN) at Huatulco station.

580 Data were used to assess living position and mortality of intertidal organisms.

581

582 Table S2. Taxonomic identity and vertical zonation of organisms used in this study.

583

584 Figure S1. Detail of organisms used in this study: a) algae *Ulva prolifera*, b) gastropod *Nerita*
585 *scabricosta*, c) gastropod *Lottia pediculus*, d) bivalve *Crassostrea corteziensis*, e) vermetid

586 Petaloconchus complicatus, f) polychaete Salmacina tribranchiata, g) crustacean Amphibalanus
587 eburneus, h) bivalve Chama coralloides, i) crustacean Megabalanus coccopoma, j) coralline
588 algae Lithophyllum sp., k) stony coral Pocillopora verrucosa and l) stony coral Pocillopora
589 damicornis, m) Saccostrea palmula.

590

591 Figure S2. Huatulco tide gauge data interpretation of land level vertical displacement and
592 tsunami amplitude after the 23 June 2020 earthquake.